

# Random walk with restart: fast solutions and applications

Hanghang Tong · Christos Faloutsos · Jia-Yu Pan

Received: 2 March 2007 / Accepted: 28 April 2007 / Published online: 4 July 2007  
© Springer-Verlag London Limited 2007

**Abstract** How closely related are two nodes in a graph? How to compute this score quickly, on huge, disk-resident, real graphs? Random walk with restart (RWR) provides a good relevance score between two nodes in a weighted graph, and it has been successfully used in numerous settings, like automatic captioning of images, generalizations to the “connection subgraphs”, personalized PageRank, and many more. However, the straightforward implementations of RWR do not scale for large graphs, requiring either quadratic space and cubic pre-computation time, or slow response time on queries. We propose fast solutions to this problem. The heart of our approach is to exploit two important properties shared by many real graphs: (a) linear correlations and (b) block-wise, community-like structure. We exploit the linearity by using low-rank matrix approximation, and the community structure by graph partitioning, followed by the Sherman–Morrison lemma for matrix inversion. Experimental results on the Corel image and the DBLP datasets demonstrate that our proposed methods achieve significant savings over the straightforward implementations: they can save *several orders* of magnitude in pre-computation and storage cost, and they achieve up to 150× speed up with 90%+ quality preservation.

**Keywords** Relevance score · Random walk with restart · Graph Mining

---

H. Tong (✉) · C. Faloutsos · J.-Y. Pan  
Carnegie Mellon University, Pittsburgh, PA, USA  
e-mail: htong@cs.cmu.edu

C. Faloutsos  
e-mail: christos@cs.cmu.edu

J.-Y. Pan  
e-mail: jypan@cs.cmu.edu

## 1 Introduction

Defining the relevance score between two nodes is one of the fundamental building blocks in graph mining [2, 7, 20, 21, 24, 28]. One very successful technique is based on random walk with restart (RWR). RWR has been receiving increasing interest from both the application and the theoretical point of view (see Sect. 5 for detailed review). An important research challenge is its speed, especially for large graphs.

Mathematically, RWR requires a matrix inversion. There are two straightforward solutions, none of which is scalable for large graphs: The first one is to pre-compute and store the inversion of a matrix (“*PreCompute*” method); the second one is to compute the matrix inversion on the fly, say, through power iteration (“*OnTheFly*” method). The first method is fast on query time, but prohibitive on space (quadratic on the number of nodes on the graph), while the second is slow on query time.

Here we propose a novel solution to this challenge. Our approach, B\_LIN, takes the advantage of two properties shared by many real graphs: (a) the block-wise, community-like structure, and (b) the linear correlations across rows and columns of the adjacency matrix. The proposed method carefully balances the off-line pre-processing cost (both the CPU cost and the storage cost), with the response quality (with respect to both the accuracy and the response time). Compared to *PreCompute*, it only requires pre-computing and storing the low-rank approximation of a large but sparse matrix, and the inversion of some small size matrices. Compared with *OnTheFly*, it only need a few matrix–vector multiplication operations in on-line response process.

The main contributions of the paper are as follows:

- A novel, fast, and practical solution (B\_LIN and its derivatives, NB\_LIN and BB\_LIN);
- Theoretical justification and analysis, giving an error bound for NB\_LIN;
- Extensive experiments on several typical applications, with real data.

The proposed method is operational, with careful design and numerous optimizations. Our experimental results show that, in general, it preserves 90%+ quality, while (a) saves several orders of magnitude of pre-computation and storage cost over *PreCompute*, and (b) it achieves up to  $150 \times$  speedup on query time over *OnTheFly*. For the DBLP author-conference dataset, with light pre-computational and storage cost, it achieves up to  $1,800 \times$  speedup with no quality loss. Figure 1a shows some results for the auto-captioning application as in [25]. Figure 1b shows some results for the neighborhood formation application as in [28].

The rest of the paper is organized as follows: the proposed method is presented in Sect. 2; the justification and the analysis are provided in Sect. 3. The experimental results are presented in Sect. 4. The related work is given in Sect. 5. Finally, we conclude the paper in Sect. 6.

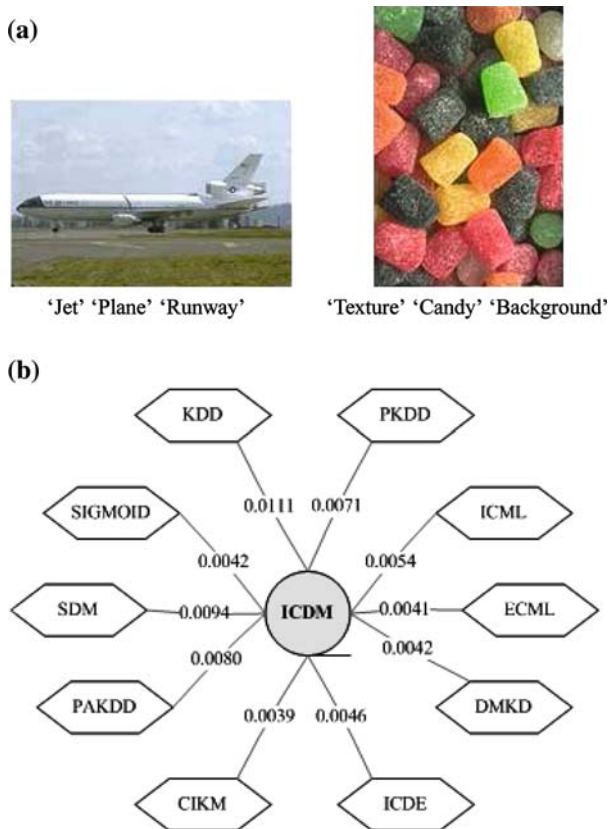
## 2 Fast RWR

### 2.1 Preliminary

Table 1 gives a list of symbols used in this paper.

Random walk with restart is defined as Eq. (1) [25]: consider a random particle that starts from node  $i$ . The particle iteratively transmits to its neighborhood with the probability that is proportional to their edge weights. Also at each step, it has some probability  $c$  to return to the node  $i$ . The relevance score of node  $j$  wrt node  $i$  is defined as the steady-state probability

**Fig. 1** Application examples by RWR: **a** Automatic image captioning. The proposed method and *OnTheFly* output the same result within 0.04 and 4.5 s, respectively. **b** Neighborhood formulation. Find the ten most related conferences for ICDM. The proposed method and *OnTheFly* output the same result within 0.013 and 23.97 s, respectively



$r_{i,j}$  that the particle will finally stay at node  $j$  [25].

$$\vec{r}_i = c\tilde{\mathbf{W}}\vec{r}_i + (1 - c)\vec{e}_i \quad (1)$$

Equation (1) defines a linear system problem, where  $\vec{r}_i$  is determined by

$$\begin{aligned} \vec{r}_i &= (1 - c)(I - c\tilde{\mathbf{W}})^{-1}\vec{e}_i \\ &= (1 - c)\mathbf{Q}^{-1}\vec{e}_i \end{aligned} \quad (2)$$

The relevance score defined by RWR has many good properties: compared with those pair-wise metrics, it can capture the global structure of the graph [14]; compared with those traditional graph distances (such as shortest path, maximum flow etc.), it can capture the multi-facet relationship between two nodes [29].

One of the most widely used ways to solve random walk with restart is the iterative method, iterating Eq. (1) until convergence, that is, until the  $L_2$  norm of successive estimates of  $\vec{r}_i$  is below our threshold  $\xi_1$ , or a maximum iteration step  $m$  is reached. In the paper, we refer it as *OnTheFly* method. *OnTheFly* does not require pre-computation and additional storage cost. Its online response time is linear to the iteration number and the number of edges,<sup>1</sup> which might be undesirable when (near) real-time response is a crucial factor while the dataset is large. A nice observation of [28] is that the distribution of  $\vec{r}_i$  is highly skewed. Based on

<sup>1</sup> Here, we store  $\tilde{\mathbf{W}}$  in a sparse format.

**Table 1** Symbols

Symbol	Definition
$\mathbf{W} = [w_{i,j}]$	The weighted graph, $1 \leq i, j \leq n$
$\tilde{\mathbf{W}}$	The normalized weighted matrix associated with $\mathbf{W}$
$\tilde{\mathbf{W}}_1$	The within-partition matrix associated with $\tilde{\mathbf{W}}$
$\tilde{\mathbf{W}}_2$	The cross-partition matrix associated with $\tilde{\mathbf{W}}$
$\mathbf{Q}$	The system matrix associated with $\mathbf{W}$ : $\mathbf{Q} = \mathbf{I} - c\tilde{\mathbf{W}}$
$\mathbf{D}$	$n \times n$ matrix, $D_{i,i} = \sum_j w_{i,j}$ and $D_{i,j} = 0$ for $i \neq j$
$\mathbf{U}$	$n \times t$ node-concept matrix
$\mathbf{S}$	$t \times t$ concept-concept matrix
$\mathbf{V}$	$t \times n$ concept-node matrix
$\mathbf{0}$	a block matrix, whose elements are all zeros
$\vec{e}_i$	$n \times 1$ starting vector, the $i$ th element 1 and 0 for others
$\vec{r}_i = [r_{i,j}]$	$n \times 1$ ranking vector, $r_{i,j}$ is the relevance score of node $j$ wrt node $i$
$c$	The restart probability, $0 \leq c \leq 1$
$n$	The total number of the nodes in the graph
$k$	The number of partitions
$t$	The rank of low-rank approximation
$m$	The maximum iteration number
$\xi_1$	The threshold to stop the iteration process
$\xi_2$	The threshold to sparse the matrix

this observation, combined with the factor that many real graphs has block-wise/community structure, the authors in [28] proposed performing RWR only on the partition that contains the starting point  $i$  (method *Blk*). However, for all data points outside the partition,  $r_{i,j}$  is simply set 0. In other words, *Blk* outputs a local estimation of  $\vec{r}_i$ .

On the other hand, it can be seen from Eq. (2) that the system matrix  $\mathbf{Q}$  defines all the steady-state probabilities of random walk with restart. Thus, if we can pre-compute and store  $\mathbf{Q}^{-1}$ , we can get  $\vec{r}_i$  real-time (We refer to this method as *PreCompute*.) However, pre-computing and storing  $\mathbf{Q}^{-1}$  is impractical when the dataset is large, since it requires quadratic space and cubic pre-computation.<sup>2</sup>

On the other hand, linear correlations exist in many real graphs, which means that we can approximate  $\tilde{\mathbf{W}}$  by low-rank approximation. This property allows us to approximate  $\mathbf{Q}^{-1}$  very efficiently. Moreover, this enables a global estimation of  $\vec{r}_i$ , unlike the local estimation obtained by *Blk*. However, due to the low rank approximation, such kind of estimation is conducted at a coarse resolution.

## 2.2 Algorithm

In summary, the skewed distribution of  $\vec{r}_i$  and the block-wise structure of the graph lead to a local/fine resolution estimation; the linear correlations of the graph lead to a global/coarse

<sup>2</sup> Even if we use *OnTheFly* to compute each column of  $\mathbf{Q}^{-1}$ , the pre-computation cost is still linear to the number of node  $n$ .

**Table 2** B\_LIN

**Input:** The normalized weighted matrix  $\tilde{\mathbf{W}}$  and the starting vector  $\vec{e}_i$

**Output:** The ranking vector  $\vec{r}_i$

**Pre-Computational Stage(Off-Line):**

p1. Partition the graph into  $k$  partitions by METIS [19];

p2. Decompose  $\tilde{\mathbf{W}}$  into two matrices:  $\tilde{\mathbf{W}} = \tilde{\mathbf{W}}_1 + \tilde{\mathbf{W}}_2$  according to the partition result, where  $\tilde{\mathbf{W}}_1$  contains all within-partition links and  $\tilde{\mathbf{W}}_2$  contains all cross-partition links;

p3. Let  $\tilde{\mathbf{W}}_{1,i}$  be the  $i^{th}$  partition, denote  $\tilde{\mathbf{W}}_1$  as equation(3);

p4. Compute and store  $\mathbf{Q}_{1,i}^{-1} = (\mathbf{I} - c\tilde{\mathbf{W}}_{1,i})^{-1}$  for each partition  $i$ ;

p5. Do low-rank approximation for  $\tilde{\mathbf{W}}_2 = \mathbf{U}\mathbf{S}\mathbf{V}$ ;

p6. Define  $\mathbf{Q}_1^{-1}$  as equation (4). Compute and store  $\tilde{\mathbf{\Lambda}} = (\mathbf{S}^{-1} - c\mathbf{V}\mathbf{Q}_1^{-1}\mathbf{U})^{-1}$ .

**Query Stage (On-Line):**

q1. Output  $\vec{r}_i = (1 - c)(\mathbf{Q}_1^{-1}\vec{e}_i + c\mathbf{Q}_1^{-1}\mathbf{U}\tilde{\mathbf{\Lambda}}\mathbf{V}\mathbf{Q}_1^{-1}\vec{e}_i)$ .

resolution estimation. In this paper, we combine these two properties in a unified manner. The proposed algorithm, B\_LIN is shown in Table 2. A pictorial description of B\_LIN is given in Fig. 2.

$$\tilde{\mathbf{W}}_1 = \begin{pmatrix} \tilde{\mathbf{W}}_{1,1} & \mathbf{0} & \dots & \mathbf{0} \\ \mathbf{0} & \tilde{\mathbf{W}}_{1,2} & \dots & \mathbf{0} \\ \dots & \dots & \dots & \dots \\ \mathbf{0} & \dots & \mathbf{0} & \tilde{\mathbf{W}}_{1,k} \end{pmatrix} \quad (3)$$

$$\mathbf{Q}_1^{-1} = \begin{pmatrix} \mathbf{Q}_{1,1}^{-1} & \mathbf{0} & \dots & \mathbf{0} \\ \mathbf{0} & \mathbf{Q}_{1,2}^{-1} & \dots & \mathbf{0} \\ \dots & \dots & \dots & \dots \\ \mathbf{0} & \dots & \mathbf{0} & \mathbf{Q}_{1,k}^{-1} \end{pmatrix} \quad (4)$$

### 2.3 Normalization on $\mathbf{W}$

B\_LIN takes the normalized matrix  $\tilde{\mathbf{W}}$  as the input. There are several ways to normalize the weighted matrix  $\mathbf{W}$ . The most natural way might be by row normalization [25]. Complementarily, the authors in [30] propose using the normalized graph Laplacian ( $\tilde{\mathbf{W}} = \mathbf{D}^{-1/2}\mathbf{W}\mathbf{D}^{-1/2}$ ). In [29], the authors also propose penalizing the famous nodes before row normalization for social network.

It should be pointed out that all the above normalization methods can be fitted into the proposed B\_LIN. However, in this paper, we will focus on the normalized graph Laplacian<sup>3</sup> for the following reasons:

<sup>3</sup> It should be pointed out that strictly speaking,  $\vec{r}_i$  is no longer a probability distribution. However, for all the applications we cover in this paper, it does not matter since what we need is a relevance score. On the other hand, we can always normalized  $\vec{r}_i$  to get a probability distribution.

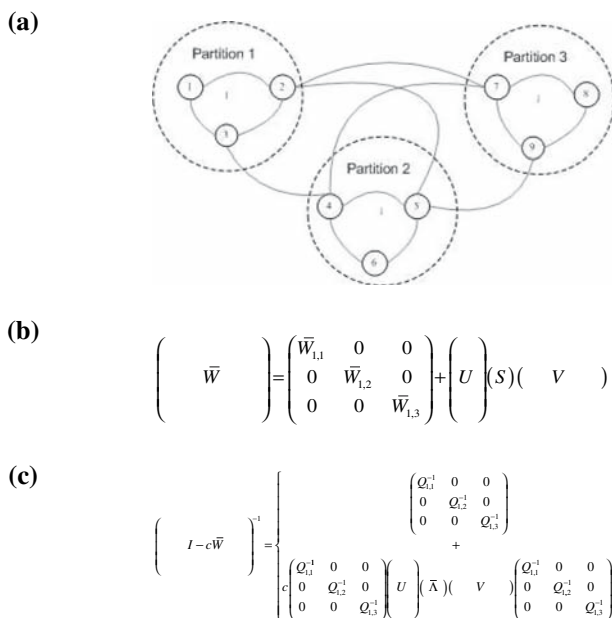


**Fig. 2** A pictorial description of B\_LIN: **a** Original weighted graph, consisting of three partitions, which are indicated by the *dash circles*. **b** Decompose original weighted graph into within-partition matrix ( $\bar{W}_1$ ), which is block-diagonal, and cross-partition matrix, which is approximated by low-rank approximation ( $U$ ,  $S$ , and  $V$ ). **c** Approximate the inverse of  $(I - c\bar{W})$  by the inversion of a few small size matrices ( $Q_{1,1}$ ,  $Q_{1,2}$ ,  $Q_{1,3}$  and  $\tilde{\Lambda}$ ), which can be pre-computed and stored more efficiently

- For real applications, these normalization methods often lead to very similar results. For cross-media correlation discovery, our experiments demonstrate that normalized graph Laplacian actually outperforms the row normalization method, which is originally proposed by the authors in [25]
- Unlike the other two methods, normalized graph Laplacian outputs the symmetric relevance score (that is  $r_{i,j} = r_{j,i}$ ), which is a desirable property for some applications.
- The normalized graph Laplacian is symmetric, and it leads to a symmetric  $Q_1$ , which will save 50% storage cost.
- It might be difficult to develop an error bound for B\_LIN in the general case. However, as we will show in Sect. 3.3, it is possible to develop an error bound for the simplified version (NB\_LIN) of B\_LIN, which also benefits from the symmetric property of the normalized graph Laplacian.

## 2.4 Partition number $k$ : case study

The partition number  $k$  balances the complexity of  $\tilde{W}_1$  and  $\tilde{W}_2$ . We will evaluate different values for  $k$  in the experiment section. Here, we investigate two extreme cases of  $k$ .

First, if  $k = 1$ , we have  $\tilde{W}_1 = \tilde{W}$  and  $\tilde{W}_2 = \mathbf{0}$ . Then, B\_LIN is just equivalent to the *PreCompute* method.

On the other hand, if  $k = n$ , we have  $\tilde{W}_1 = \mathbf{0}$  and  $\tilde{W}_2 = \tilde{W}$ . In this case,  $Q_1 = I$  and we have the following simplified version of B\_LIN as in Table 3. We refer it as NB\_LIN.

**Table 3** NB\_LIN

---

<b>Input:</b> The normalized weighted matrix $\tilde{\mathbf{W}}$ and the starting vector $\tilde{\mathbf{e}}_i$
<b>Output:</b> The ranking vector $\tilde{\mathbf{r}}_i$
<b>Pre-Computational Stage(Off-Line):</b>
p1. Do low-rank approximation for $\tilde{\mathbf{W}} = \mathbf{USV}$ ;
p2. Compute and store $\tilde{\mathbf{A}} = (\mathbf{S}^{-1} - c\mathbf{VU})^{-1}$ .
<b>Query Stage (On-Line):</b>
q1. Output $\tilde{\mathbf{r}}_i = (1 - c)(\tilde{\mathbf{e}}_i + c\mathbf{U}\tilde{\mathbf{A}}\mathbf{V}\tilde{\mathbf{e}}_i)$ .

---

**Table 4** BB\_LIN

---

<b>Input:</b> The normalized weighted matrix $\tilde{\mathbf{W}}$ and the starting vector $\tilde{\mathbf{e}}_i$ as Eq. 5
<b>Output:</b> The ranking vector $\tilde{\mathbf{r}}_i$ as Eq. 5
<b>Pre-Computational Stage(Off-Line):</b>
p1. Compute and store $\tilde{\mathbf{A}} = (\mathbf{I} - c^2\mathbf{M}^T\mathbf{M})^{-1}$ ;
<b>Query Stage (On-Line):</b>
q1. $\tilde{\mathbf{r}}_{i,1} = (1 - c)(\tilde{\mathbf{e}}_{i,1} + c^2\mathbf{M}\tilde{\mathbf{A}}\mathbf{M}^T\tilde{\mathbf{e}}_{i,1} + c\mathbf{M}\tilde{\mathbf{A}}\tilde{\mathbf{e}}_{i,2})$
q2. $\tilde{\mathbf{r}}_{i,2} = (1 - c)(c\tilde{\mathbf{A}}\mathbf{M}^T\tilde{\mathbf{e}}_{i,1} + \tilde{\mathbf{A}}\tilde{\mathbf{e}}_{i,2})$
q3. Output $\tilde{\mathbf{r}}_i = (\tilde{\mathbf{r}}_{i,1}, \tilde{\mathbf{r}}_{i,2})^T$ .

---

An application of random walk with restart is neighborhood formulation in the bipartite graph [28]. Suppose there are  $n_1$  and  $n_2$  nodes for each type of objects in the bipartite graph;  $\mathbf{M}$  is the  $n_1 \times n_2$  bipartite matrix. The normalized weighted matrix, the starting vector and the ranking vector have the following format:

$$\tilde{\mathbf{W}} = \begin{pmatrix} \mathbf{0} & \mathbf{M} \\ \mathbf{M}^T & \mathbf{0} \end{pmatrix} \quad \tilde{\mathbf{r}}_i = \begin{pmatrix} \tilde{\mathbf{r}}_{i,1} \\ \tilde{\mathbf{r}}_{i,2} \end{pmatrix} \quad \tilde{\mathbf{e}}_i = \begin{pmatrix} \tilde{\mathbf{e}}_{i,1} \\ \tilde{\mathbf{e}}_{i,2} \end{pmatrix} \quad (5)$$

As a direct application of NB\_LIN, we have the following fast algorithm (BB\_LIN) for one class of bipartite graph when  $n_1 \gg n_2$  as in Table 4.

## 2.5 Low-rank approximation on $\tilde{\mathbf{W}}_2$

One natural choice to do low-rank approximation on  $\tilde{\mathbf{W}}_2$  is by eigen-value decomposition:<sup>4</sup>

$$\tilde{\mathbf{W}}_2 = \mathbf{USU}^T \quad (6)$$

where each column of  $\mathbf{U}$  is the eigen-vector of  $\tilde{\mathbf{W}}_2$  and  $\mathbf{S}$  is a diagonal matrix, whose diagonal elements are eigen-values of  $\tilde{\mathbf{W}}_2$ .

The advantage of eigen-value decomposition is that it is ‘optimal’ in terms of reconstruction error. Also, since  $\mathbf{V} = \mathbf{U}^T$  in this situation, we can save 50% storage cost. However, one potential problem is that it might lose the sparsity of original matrix  $\tilde{\mathbf{W}}_2$ . Also, when  $\tilde{\mathbf{W}}_2$  is large, doing eigen-value decomposition itself might be time-consuming.

To address this issue, in this paper, we also propose the following heuristic to do low-rank approximation as in Table 5. Its basic idea is that, firstly, construct  $\mathbf{U}$  by partitioning  $\tilde{\mathbf{W}}_2$ ; and

<sup>4</sup> if the other two normalization methods are used, we can do singular vector decomposition instead.

**Table 5** Low rank approximation by partition**Input:** The cross-partition matrix  $\tilde{\mathbf{W}}_2$  and  $t$ **Output:** Low rank approximation of  $\tilde{\mathbf{W}}_2$ :  $\mathbf{U}, \mathbf{S}, \mathbf{V}$ 

1. Partition  $\tilde{\mathbf{W}}_2$  into  $t$  partitions;
2. Construct an  $n \times t$  matrix  $\mathbf{U}$ . The  $i$ th column of  $\mathbf{U}$  is the sum of all the columns of  $\tilde{\mathbf{W}}_2$  that belong to the  $i$ th partition;
3. Compute  $\mathbf{S} = (\mathbf{U}^T \mathbf{U})^{-1}$ ;
4. Compute  $\mathbf{V} = \mathbf{U}^T \tilde{\mathbf{W}}_2$ .

then use the projection of  $\tilde{\mathbf{W}}_2$  on the sub-space spanned by the columns of  $\mathbf{U}$  as the low-rank approximation.

### 3 Justification and analysis

#### 3.1 Correctness

Here, we present a brief proof of the proposed algorithms

##### 3.1.1 B\_LIN

**Lemma 1** *If  $\tilde{\mathbf{W}} = \tilde{\mathbf{W}}_1 + \mathbf{USV}$  holds, B\_LIN outputs exactly the same result as PreCompute.*

*Proof* Since  $\tilde{\mathbf{W}}_1$  is a block-diagonal matrix. Based on Eq. (3) and (4), we have

$$(\mathbf{I} - c\tilde{\mathbf{W}}_1)^{-1} = \mathbf{Q}_1^{-1} \quad (7)$$

Then, based on the Sherman–Morrison lemma [26], we have

$$\begin{aligned} \tilde{\Lambda} &= (\mathbf{S}^{-1} - c\mathbf{V}\mathbf{Q}_1^{-1}\mathbf{U})^{-1} \\ (\mathbf{I} - c\tilde{\mathbf{W}})^{-1} &= (\mathbf{I} - c\tilde{\mathbf{W}}_1 - c\mathbf{USV})^{-1} \\ &= \mathbf{Q}_1^{-1} + c\mathbf{Q}_1^{-1}\mathbf{U}\tilde{\Lambda}\mathbf{V}\mathbf{Q}_1^{-1} \\ \vec{r}_i &= (1 - c)(\mathbf{Q}_1^{-1}\vec{e}_i + c\mathbf{Q}_1^{-1}\mathbf{U}\tilde{\Lambda}\mathbf{V}\mathbf{Q}_1^{-1}\vec{e}_i) \end{aligned}$$

which completes the proof of Lemma 1. It can be seen that the only approximation of B\_LIN comes from the low-rank approximation for  $\tilde{\mathbf{W}}_2$ .

We can also interpret B\_LIN from the perspective of latent semantic/concept space. By low-rank approximation on  $\tilde{\mathbf{W}}_2$ , we actually introduce a  $t \times t$  latent concept space by  $\mathbf{S}$ . Furthermore, if we treat the original  $\tilde{\mathbf{W}}$  as an  $n \times n$  node space,  $\mathbf{U}$  and  $\mathbf{V}$  actually define the relationship between these two spaces ( $\mathbf{U}$  for node–concept relationship and  $\mathbf{V}$  for concept–node relationship). Thus, it can be seen that, instead of doing random walk with restart on the original whole node space, B\_LIN decomposes it into the following simple steps:

- (1) Doing RWR within the partition that contains the starting point (multiply  $\vec{e}_i$  by  $\mathbf{Q}_1^{-1}$ );
- (2) Jumping from node-space to latent concept space (multiply the result of (1) by  $\mathbf{V}$ );
- (3) Doing RWR within the latent concept space (multiply the result of (2) by  $\tilde{\Lambda}$ );
- (4) Jumping back to the node space (multiply the result of (3) by  $\mathbf{U}$ );
- (5) Doing RWR within each partition until convergence (multiply the result of (4) by  $\mathbf{Q}_1^{-1}$ ).



### 3.1.2 NB\_LIN

**Lemma 2** If  $\tilde{\mathbf{W}} = \mathbf{USV}$  holds, NB\_LIN outputs exactly the same result as PreCompute.

*Proof* Taking  $\tilde{\mathbf{W}}_1 = \mathbf{0}$  and  $\mathbf{Q}_1 = \mathbf{I}$ , by applying Lemma 1, we directly complete the proof of Lemma 2.

### 3.1.3 BB\_LIN

**Lemma 3** BB\_LIN outputs exactly the same result as PreCompute.

*Proof* Substituting Eq. (5) into Eq. (2), we have

$$\begin{aligned}\vec{r}_{i,1} &= (1 - c)(\mathbf{I} - c^2\mathbf{MM}^T)^{-1}(c\mathbf{M}\vec{e}_{i,2} + \vec{e}_{i,1}) \\ \vec{r}_{i,2} &= (1 - c)(\mathbf{I} - c^2\mathbf{M}^T\mathbf{M})^{-1}(c\mathbf{M}^T\vec{e}_{i,1} + \vec{e}_{i,2})\end{aligned}$$

Solving  $\vec{r}_{i,2}$  directly completes the proof of 'q2' in Table 4.

Define a new RWR, which takes (1)  $(c\mathbf{M}\vec{e}_{i,2} + \vec{e}_{i,1})$  as the new starting vector; (2)  $(c\mathbf{MM}^T)$  as the new normalized weighted matrix; and (3)  $(\mathbf{M}(c\mathbf{I})\mathbf{M}^T)$  as the low-rank approximation. Applying Lemma 2 to this RWR, we complete the proof for 'q1' in Table 4, which in turn completes the proof of Lemma 3.

## 3.2 Computational and storage cost

In this section, we make a brief analysis for the proposed algorithms in terms of computational and storage cost. For the limited space, we only provide the result for B\_LIN.

### 3.2.1 On-line computational cost

It is not hard to see that, at the on-line query stage of B\_LIN (Table 2, step q1), we only need a few matrix-vector multiplication operations as shown in Eq. (8). Therefore, B\_LIN is capable of meeting the (near) real-time response requirement.

$$\begin{aligned}\vec{r}_0 &\leftarrow \mathbf{Q}_1^{-1}\vec{e}_i \\ \vec{r}_i &\leftarrow \mathbf{V}\vec{r}_0 \\ \vec{r}_i &\leftarrow \tilde{\Lambda}\vec{r}_i \\ \vec{r}_i &\leftarrow \mathbf{U}\vec{r}_i \\ \vec{r}_i &\leftarrow \mathbf{Q}_1^{-1}\vec{r}_i \\ \vec{r}_i &\leftarrow (1 - c)(\vec{r}_0 + c\vec{r}_i)\end{aligned}\tag{8}$$

### 3.2.2 Pre-computational cost

The main off-line computational cost of the proposed algorithm consists of the following parts:

- (1) partitioning the whole graph;
- (2) inversion of each  $\mathbf{I} - c\tilde{\mathbf{W}}_{1,i}$  ( $i = 1, \dots, k$ );
- (3) low-rank approximation on  $\tilde{\mathbf{W}}_2$ ;
- (4) inversion of  $(\mathbf{S}^{-1} - \mathbf{VQ}_1^{-1}\mathbf{U})$ .

Thus, instead of solving the inversion of the original  $n \times n$  matrix, B\_LIN(1) inverses  $k + 1$  small matrices ( $\mathbf{Q}_{1,i}^{-1}$ ,  $i=1, \dots, k$ , and  $\tilde{\Lambda}$ ); (2) computes a low-rank approximation of a sparse  $n \times n$  matrix ( $\tilde{\mathbf{W}}_2$ ), and (3) partitions the whole graph.

### 3.2.3 Pre-storage cost

In terms of storage cost, we have to store  $k + 1$  small matrices ( $\mathbf{Q}_{1,i}^{-1}$ ,  $i = 1, \dots, k$ , and  $\tilde{\Lambda}$ ), one  $n \times t$  matrix ( $\mathbf{U}$ ) and one  $t \times n$  matrix ( $\mathbf{V}$ ). Moreover, we can further save the storage cost as shown in the following:

- An observation from all our experiments is that many elements in  $\mathbf{Q}_{1,i}^{-1}$ ,  $\mathbf{U}$  and  $\mathbf{V}$  are near zeros. Thus, an optional step is to set these elements to be zero (by the threshold  $\xi_2$ ) and to store these matrices as sparse format. For all experiments in this paper, we find that this step will significantly reduce the storage cost while almost not affecting the approximation accuracy.
- The normalized graph Laplacian is symmetric, which leads to (1) a symmetric  $\mathbf{Q}_{1,i}^{-1}$ , and (2)  $\mathbf{U} = \mathbf{V}^T$ , if eigen-value decomposition is used when computing the low-rank approximation.<sup>5</sup> By taking advantage of this symmetry property, we can further save 50% storage cost.

### 3.3 Error bound

Developing an error bound for the general case of the proposed methods is difficult. However, for NB\_LIN (Table 3), we have the following lemma:

**Lemma 4** Let  $\vec{r}$  and  $\hat{\vec{r}}$  be the ranking vectors<sup>6</sup> by PreCompute and by NB\_LIN, respectively. If NB\_LIN takes eigen-value decomposition as low-rank approximation,  $\|\vec{r} - \hat{\vec{r}}\|_2 \leq (1 - c) \sum_{i=t+1}^n \frac{1}{(1 - c\lambda_i)}$ , where  $\lambda_i$  is the  $i$ th largest eigen-value of  $\tilde{\mathbf{W}}$ .

*Proof* Taking the full eigen-value decomposition for  $\tilde{\mathbf{W}}$ :

$$\tilde{\mathbf{W}} = \sum_{i=1}^n \lambda_i \cdot u_i \cdot u_i^T = \mathbf{U} \mathbf{S} \mathbf{U}^T \quad (9)$$

where  $\lambda_i$  and  $u_i$  are the  $i$ th largest eigen-value and the corresponding eigen-vector of  $\tilde{\mathbf{W}}$ , respectively.  $\mathbf{U} = [u_1, \dots, u_n]$ , and  $\mathbf{S} = \text{diag}(\lambda_1, \dots, \lambda_n)$ . We have

$$\begin{aligned} \tilde{\Lambda} &= (\mathbf{S}^{-1} - c \mathbf{U}^T \mathbf{U})^{-1} \\ &= \sum_{i=1}^n \frac{\lambda_i}{(1 - c\lambda_i)} \cdot u_i \cdot u_i^T \end{aligned} \quad (10)$$

By Lemma 2, we have

$$\begin{aligned} \vec{r} &= (1 - c) \sum_{i=1}^n \frac{1}{(1 - c\lambda_i)} \cdot u_i \cdot u_i^T \cdot \vec{e}_i \\ \hat{\vec{r}} &= (1 - c) \sum_{i=1}^t \frac{1}{(1 - c\lambda_i)} \cdot u_i \cdot u_i^T \cdot \vec{e}_i \end{aligned} \quad (11)$$

<sup>5</sup> On the other hand, if we use partition-based low-rank approximation as in Table 5,  $\mathbf{U}$  and  $\mathbf{V}$  are usually sparse and thus can be efficiently stored.

<sup>6</sup> Here, we ignore the low script  $i$  of  $\vec{r}$  and  $\hat{\vec{r}}$  for simplicity.

Thus, we have

$$\begin{aligned}
 \|\vec{r} - \hat{\vec{r}}\|_2 &= \|(1-c) \sum_{i=t+1}^n \frac{1}{(1-c\lambda_i)} \cdot u_i \cdot u_i^T \cdot \vec{e}_i\|_2 \\
 &\leq (1-c) \left\| \sum_{i=t+1}^n \frac{1}{(1-c\lambda_i)} \cdot u_i \cdot u_i^T \right\|_2 \cdot \|\vec{e}_i\|_2 \\
 &= (1-c) \sum_{i=t+1}^n \frac{1}{(1-c\lambda_i)}
 \end{aligned} \tag{12}$$

which completes the proof of Lemma 4.

## 4 Experimental results

### 4.1 Experimental setup

#### 4.1.1 Datasets

##### – CoIR

This dataset contains 5,000 images. The images are categorized into 50 groups, such as beach, bird, mountain, jewelry, sunset, etc. Each of the categories contains 100 images of essentially the same content, which serve as the ground truth. This is a widely used dataset for image retrieval. Two kinds of low-level features are used, including color moment and pyramid wavelet texture feature. We use exactly the same method as in [14] to construct the weighted graph matrix  $\mathbf{W}$ , which contains 5,000 nodes and  $\approx 774K$  edges

##### – CoMMG

This dataset is used in [25], which contains around 7,000 captioned images, each with about four captioned terms. There are in total 160 terms for captioning. In our experiments, 1,740 images are set aside for testing. The graph matrix  $\mathbf{W}$  is constructed exactly as in [25], which contains 54,200 nodes and  $\approx 354K$  edges.

##### – AP

The author-paper information of DBLP dataset [4] is used to construct the weighted graph  $\mathbf{W}$  as in Eq. (5): every author is denoted as a node in  $\mathbf{W}$ , and the edge weight is the number of co-authored papers between the corresponding two authors. On the whole, there are  $\approx 315K$  nodes and  $\approx 1,834K$  non-zero edges in  $\mathbf{W}$ .

##### – AC

The author-conference information of DBLP dataset [4] is used to construct the bipartite graph  $\mathbf{M}$ : each row corresponds to an author and each column corresponds to a conference; and the edge weight  $\mathbf{M}_{i,j}$  is the number of papers that the  $i$ th author publishes in  $j$ th conference. On the whole, there are  $\approx 291K$  nodes ( $\approx 288K$  authors and  $\approx 3K$  conferences) and  $\approx 661K$  non-zero edges in  $\mathbf{M}$ .

All the above datasets are summarized in Table 6.

**Table 6** Summary of data sets

Dataset	Number of nodes	Number of edges
CoIR	5K	$\approx 774K$
CoMMG	$\approx 52K$	$\approx 354K$
AP	$\approx 315K$	$\approx 1,834K$
AC	$\approx 291K$	$\approx 661K$

**Table 7** Summary of typical applications with different datasets

	CBIR	CMCD	Ceps	NF
CoIR	✓			✓
CoMMG		✓		
AP			✓	
AC				✓

#### 4.1.2 Applications

As mentioned before, many applications can be built upon random walk with restart. In this paper, we test the following applications:

- Center-piece subgraph discovery (CePs) [29]
- Content based image retrieval (CBIR) [14]
- Cross-modal correlation discovery (CMCD), including automatic captioning of images [25]
- Neighborhood formulation (NF) for both uni-partite graph and bipartite graph [28]

The typical datasets for these applications in the past years are summarized in Table 7.

#### 4.1.3 Parameter setting

The proposed methods are compared with *OnTheFly*, *PreCompute* and *Blk*. All these methods share three parameters:  $c$ ,  $m$  and  $\xi_1$ . we use the same parameters for CBIR as [14], that is  $c = 0.95$ ,  $m = 50$  and  $\xi_1 = 0$ . For the rest applications, we use the same setting as [25] for simplicity, that is  $c = 0.9$ ,  $m = 80$  and  $\xi_1 = 10^{-8}$ .

For B\_LIN and NB\_LIN, we take  $\xi_2 = 10^{-4}$  to sparsify  $\mathbf{Q}_1$ ,  $\mathbf{U}$ , and  $\mathbf{V}$  which further reduces storage cost. We evaluate different choices for the remaining parameters. For clarification, in the following experiments, B\_LIN is further referred as B\_LIN( $k$ ,  $t$ , Eig/Part), where  $k$  is the number of partition,  $t$  is the target rank of the low-rank approximation, and “Eig/Part” denotes the specific method for doing low-rank approximation—“Eig” for eigen-value decomposition and “Part” for partition-based low-rank approximation. Similarly, NB\_LIN is further referred as NB\_LIN( $t$ , Eig/Part), and *Blk* is further referred as *Blk*( $k$ ).

For the datasets with groundtruth (CoIR and CoMMG), we use the relative accuracy *RelAcu* as the evaluation criterion:

$$RelAcu = \frac{\widehat{Acu}}{Acu} \quad (13)$$

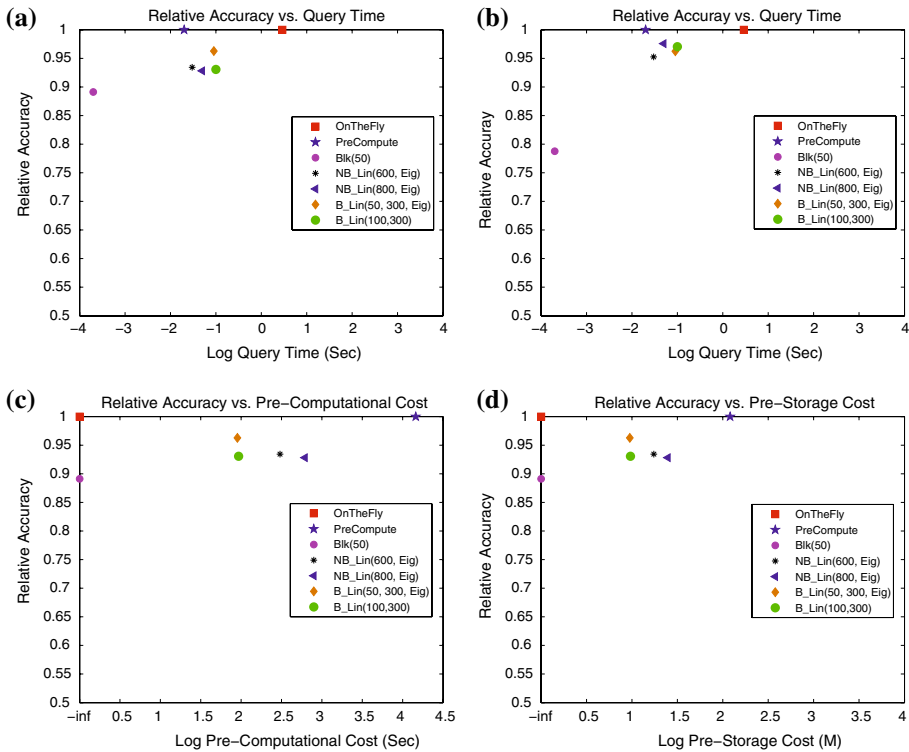


**Fig. 3** Evaluation on CoIR for CBIR: **a** accuracy (Initial) versus Log QT, **b** accuracy (RF) versus Log QT, **c** accuracy (Initial) versus Log PT and **d** accuracy (Initial) versus Log PS

where  $\widehat{Acu}$  and  $Acu$  are the accuracy values by the evaluated method and by *PreCompute*, respectively.

Another evaluation criterion is *RelScore*,

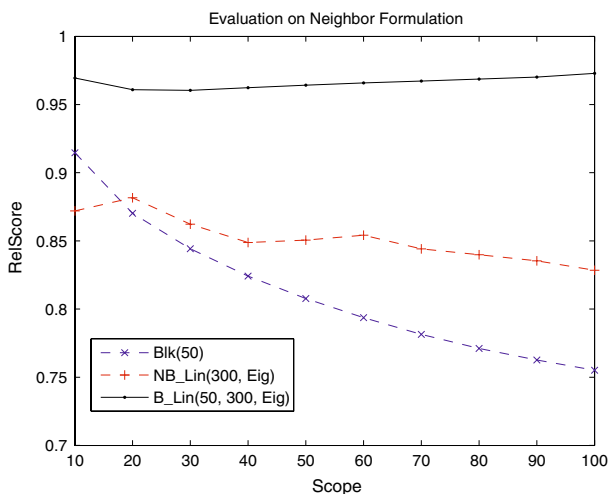
$$RelScore = \frac{\widehat{tScr}}{tScr}, \quad (14)$$

where  $\widehat{tScr}$  and  $tScr$  are the total relevance scores captured by the evaluated method and by *PreCompute*, respectively.

All the experiments are performed on the same machine with 3.2GHz CPU and 2GB memory.

#### 4.2 CoIR results

Hundred images are randomly selected from the original dataset as the query images and the precision versus scope is reported. The user feedback process is simulated as follows. In each round of relevance feedback (RF), five images that are most relevant to the query based on the current retrieval result are fed back and examined. It should be pointed out that the initial retrieval result is equivalent to that for neighborhood formulation (NF). *RelAcu* is evaluated on the first 20 retrieved images, that is, the precision within the first 20 retrieved images. In Fig. 3, the results are evaluated from three perspectives: accuracy versus query

**Fig. 4** Evaluation on CoIR for NF

time (QT), accuracy versus pre-computational time (PT) and accuracy versus pre-storage cost (PS). In the figure, the QT, PT and PS costs are in log-scale. Note that pre-computational time and storage cost are the same for both initial retrieval and relevance feedback, therefore, we only report accuracy versus pre-computational time and accuracy versus pre-storage cost for initial retrieval.

It can be seen that in all the figures, B\_LIN and NB\_LIN always lie in the upper-left zone, which indicates that the proposed methods achieve a good balance between on-line response quality and off-line processing cost. Both B\_LIN and NB\_LIN (1) achieve about one order of magnitude speedup (compared with *OnTheFly*); and (2) save one order of magnitude on pre-computational and storage cost. For example, B\_LIN(50, 300, Eig) preserves 95%+ accuracy for both initial retrieval and relevance feedback, while it (1) achieves 32 $\times$  speedup for on-line response (0.09Sec/2.91Sec), compared with *OnTheFly*; and (2) save 8 $\times$  on storage (21M/180M) and 161 $\times$  on pre-computational cost (90Sec/14,500Sec), compared with *PreCompute*. NB\_LIN(600,Eig) preserves 93%+ accuracy for both initial retrieval and relevance feedback, while it (1) achieves 97 $\times$  speedup for on-line response (0.03Sec/2.91Sec), compared with *OnTheFly*; and (2) saves 10 $\times$  on storage(17M/180M) and 48 $\times$  on pre-computational cost (303Sec/14,500Sec), compared with *PreCompute*.<sup>7</sup>

For the task of neighborhood formation (NF), Fig. 4 shows the result of RelScore versus scope. It can be seen that by exploring both the block-wise and linear correlations structure simultaneously, (1) both *Blk*(50) and NB\_LIN(50, Eig) capture most neighborhood information (for example, they both capture about 90% score for the precision on the first ten retrieved images), and (2) B\_LIN(50, 300, Eig) captures 95%+ score over the whole scope. (The improvement becomes even more significant with the increase of the scope.)

#### 4.3 CoMMG results

For this dataset, we only compare NB\_LIN with *OnTheFly* and *PreCompute*. The results are shown in Fig. 5. The  $x$ -axis of Fig. 5 is plotted in log-scale. Again, NB\_LIN lies in the upper-left zone in all the figures, which means that NB\_LIN achieves a good balance between

<sup>7</sup> We also perform experiment on BlockRank [18]. However, the result is similar with *OnTheFly*. Thus, we do not present it in this paper.

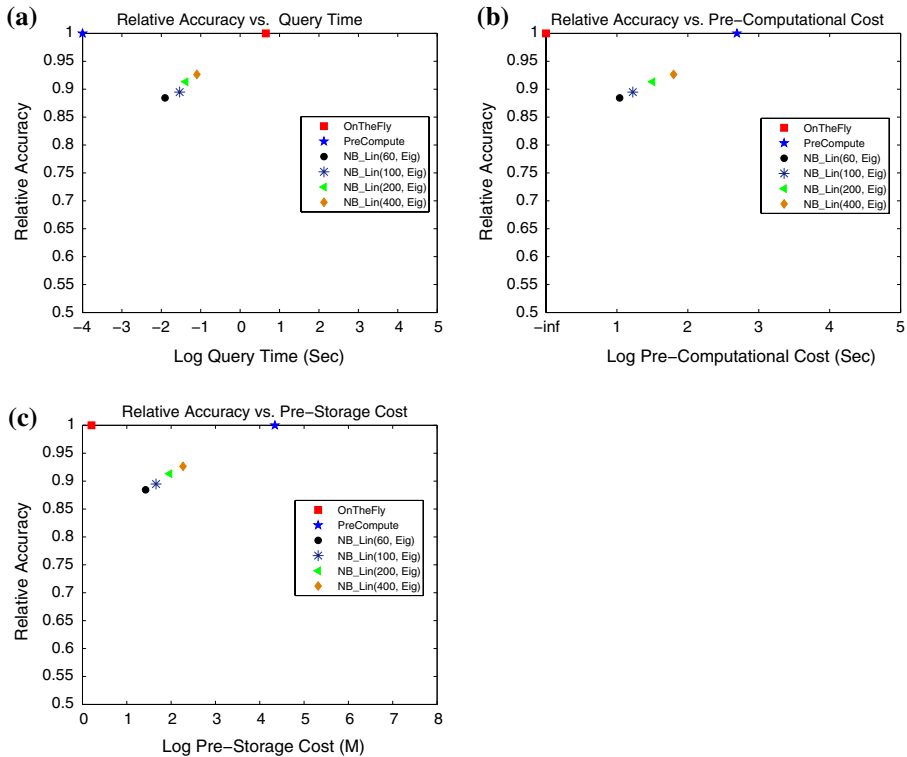


**Fig. 5** Evaluation on CoMMG for CMCD: **a** Accuracy versus Log QT, **b** Accuracy versus Log PT and **c** Accuracy versus Log PS

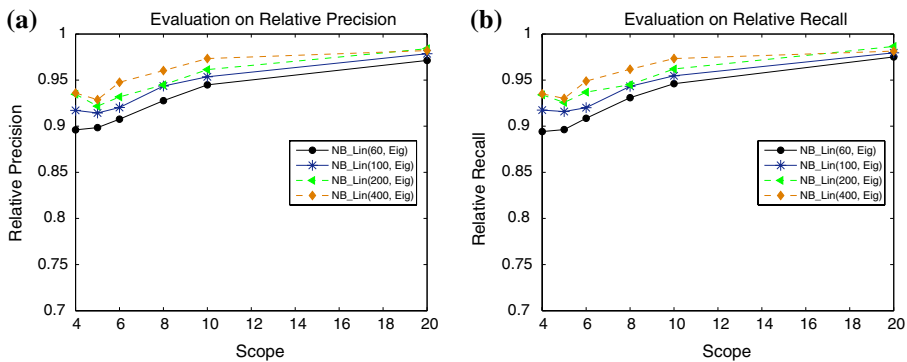


**Fig. 6** Precision/recall for CMCD: **a** relative precision and **b** relative recall

on-line quality and off-line processing cost. For example, NB\_LIN(100, Eig) preserves 91.3% quality, while it (1) achieves  $154 \times$  speedup for on-line response (0.029/4.50Sec), compared with *OnTheFly*; 2) saves 868x on storage (281/243,900M) and  $479 \times$  on pre-computational cost (46/21,951Sec), compared with *PreCompute*. The relative precision/recall versus scope is shown in Fig. 6.

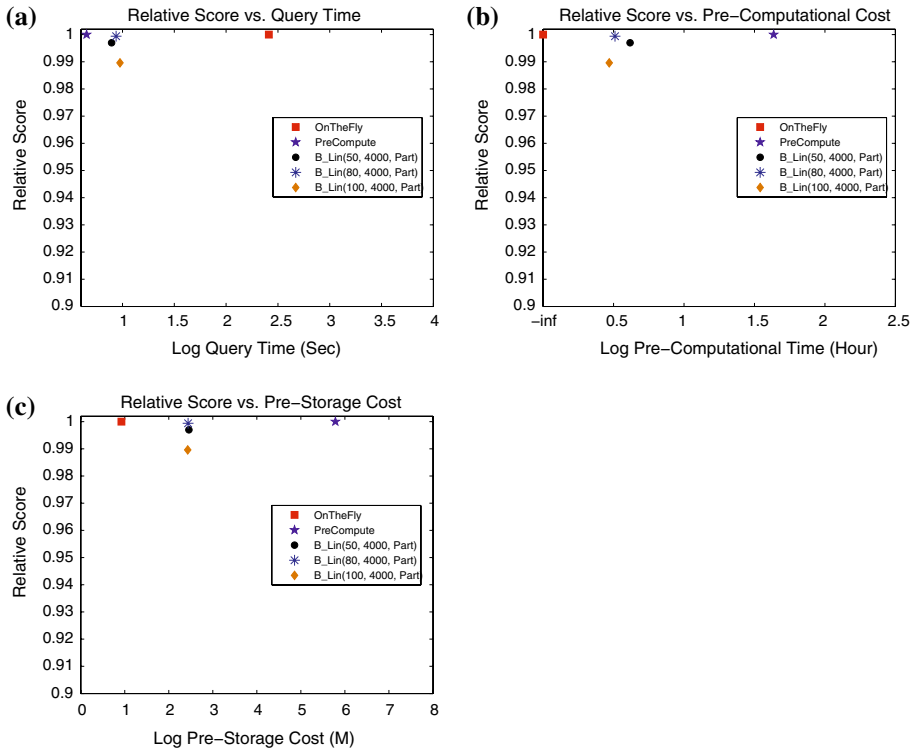


**Fig. 7** Evaluation on AP for Ceps: **a** accuracy versus Log QT, **b** accuracy versus Log PT and **c** accuracy versus Log QS

#### 4.4 AP results

This dataset is used to evaluate Ceps as in [29]. B\_LIN is used to generate 1,000 candidates, which are further fed to the original Ceps Algorithm [29] to generate the final center-piece subgraphs. We fix the number of query nodes to be 3 and the size of the subgraph to be 20. RelScore is measured by “Important Node Score” as in [29]. The result is shown in Fig. 7.

Again, B\_LIN lies in the upper-left zone in all the figures, which means that B\_LIN achieves a good balance between on-line quality and off-line processing cost. For example, B\_LIN(100, 4000, Part) preserves 98.9% quality, while it (1) achieves  $27\times$  speedup for on-line response (9.45/258.2Sec), compared with *OnTheFly*; (2) saves  $2264\times$  on storage (269/609,020M) and  $214\times$  on pre-computational cost (8.7/1875Hour), compared with *PreCompute*.

#### 4.5 AC results

For this dataset, the number of conferences (3K) is much less than that of the authors (228K). We evaluate BB\_LIN for the following four tasks:

- **C\_C**: Given a conference, find its most related conferences
- **C\_A**: Given a conference, find its most related authors
- **A\_A**: Given an author, find its most related authors



**Table 8** Evaluation on AC for NF

Method	QT (Sec)	PT(Sec)	PS(M)
<i>OnTheFly</i>	23.97	0	6.7
<i>PreCompute</i>	0.001	6,990,648	626,250
BB_LIN(C, A)	0.097	20.50	56
BB_LIN(C, C)	0.013	20.50	56
BB_LIN(A, C)	0.035	20.50	56
BB_LIN(A, A)	0.13	20.50	56

- **A\_C**: Given an author, find its most related conferences

On this application, BB\_LIN preserves 100% accuracy for all the tasks. Thus, in Table 8, we only report Query time (QT), Pre-computational time (PT), and Pre-storage cost (PS). Note that the query time for BB\_LIN might differ for the different tasks. For clarification, BB\_LIN is further referred as BB\_LIN(C/A C/A). (For example, BB\_LIN(C, A) denotes using BB\_LIN for C\_A task.)

As shown in Table 8, BB\_LIN can achieve up to 3 orders of magnitude speedup, with light off-line computational and storage cost (20.5Sec for pre-computation and 56M for pre-storage). For example, it achieves  $180\times$  speedup for **A\_A** (0.13/23.98Sec) and  $1,800\times$  speedup for **C\_C** (0.013/23.98Sec).

## 5 Related work

In this section, we briefly review related work, which can be categorized into three groups: (1) random walk related methods; (2) graph partitioning methods and (3) the methods for low-rank approximation.

*Random walk related methods.* There are several methods similar to RWR, including electricity-based method [31], graph-based Semi-supervised learning [7,30] and so on. Exact solution of these methods usually requires the inversion of a matrix which is often diagonal dominant and of big size. Other methods sharing this requirement include regularized regression, Gaussian process regression [27], and so on. Existing fast solution for RWR include Hub-vector decomposition based [16]; block structure based [18,28]; fingerprint based [9], and so on. Many applications take random walk and related methods as the building block, including PageRank [23], personalized PageRank [13], SimRank [15], neighborhood formulation in bipartite graphs [28], content-based image retrieval [14], cross modal correlation discovery [25], the BANKS system [2], ObjectRank [3], RelationalRank [10], and so on.

*Graph partition and clustering.* Several algorithms have been proposed for graph partition and clustering, e.g., METIS [19], spectral clustering [22], flow simulation [8], co-clustering [6], and the betweenness based method [11]. It should be pointed out that the proposed method is orthogonal to the partition method.

*Low-rank approximation.* One of the widely used techniques is singular vector decomposition (SVD) [12], which is the base for a lot of powerful tools, such as latent semantic index (LSI) [5], principle component analysis (PCA) [17], and so on. For symmetric matrices, a complementary technique is the eigen-value decomposition [12]. More recently, CUR decomposition has been proposed for sparse matrices [1].

## 6 Conclusions

In this paper, we propose a fast solution for computing the random walk with restart. The main contributions of the paper are as follows:

- The design of B\_LIN and its derivative, NB\_LIN. These methods take advantages of the block-wise structure and linear correlations in the adjacency matrix of real graphs, using the Sherman–Morrison Lemma.
- The proof of an error bound for NB\_LIN. To our knowledge, this is the first attempt to derive an error bound for fast random walk with restart.
- Extensive experiments are performed on several real datasets, on typical applications. The results demonstrate that our proposed algorithm can nicely balance the off-line processing cost and the on-line response quality. In most cases, our methods preserve 90%+ quality, with dramatic savings on the pre-computation cost and the query time.
- A fast solution (BB\_LIN) for one particular class of bipartite graphs. Our method achieves up to  $1,800 \times$  speedup with light pre-computational and storage cost, without suffering quality loss.

Future work includes exploring error bounds for the general case of B\_LIN and performing comparative experiments with other candidate solutions, such as [9, 16].

**Acknowledgments** This material is based upon work supported by the National Science Foundation under Grants No. IIS-0326322 IIS-0534205 and under the auspices of the US Department of Energy by University of California Lawrence Livermore National Laboratory under contract No. W-7405-ENG-48. This work is also partially supported by the Pennsylvania Infrastructure Technology Alliance (PITA), an IBM Faculty Award, a Yahoo Research Alliance Gift, with additional funding from Intel, NTT and Hewlett-Packard. Any opinions, findings, and conclusions or recommendations expressed in this material are those of the author(s) and do not necessarily reflect the views of the National Science Foundation, or other funding parties.

## References

1. Achlioptas D, McSherry F (2001) Fast computation of low rank matrix approximation. In: STOC
2. Aditya B, Bhalotia G, Chakrabarti S, Hulgeri A, Nakhe C, Parag SS (2002) Banks: Browsing and keyword searching in relational databases. In: VLDB, pp 1083–1086
3. Balmin A, Hristidis V, Papakonstantinou Y (2004) Objectrank: Authority-based keyword search in databases. In: VLDB, **564**, 564–575
4. <http://www.informatik.uni-trier.de/ley/db/>
5. Deerwester S, Dumais S, Landauer T, Furnas G, Harshman R, (1990) Indexing by latent semantic analysis. *J Am Soc Inform Sci* **41**(6), 391–407
6. Dhillon IS, Mallela S, Modha DS (2003) Information-theoretic co-clustering. In: The ninth ACM SIG-KDD international conference on knowledge discovery and data mining (KDD 03), Washington, DC, August 24–27
7. Faloutsos C, McCurley KS, Tomkins A (2004) Fast discovery of connection subgraphs. In: KDD, pp 118–127
8. Flake G, Lawrence S, Giles C (2000) Efficient identification of web communities. In: KDD, pp 150–160
9. Fogaras D, Racz B (2004) Towards scaling fully personalized pagerank. In: Proc. WAW, pp 105–117
10. Geerts F, Mannila H, Terzi E (2004) Relational link-based ranking. In: VLDB, pp 552–563
11. Girvan M, Newman MEJ (2002) Community structure in social and biological networks. *Proc Natl Acad Sci* **78**21–7826
12. Golub G, Loan C (1996) Matrix computation. Johns Hopkins
13. Haveliwala TH (2002) Topic-sensitive pagerank. WWW, pp 517–526
14. He J, Li M, Zhang H, Tong H, Zhang C (2004) Manifold-ranking based image retrieval. In: ACM Multimedia, pp 9–16
15. Jeh G, Widom J (2002) Simrank: A measure of structural-context similarity. In: KDD, pp 538–543
16. Jeh G, Widom J (2003) Scaling personalized web search. In: WWW

17. Jolliffe I (2002) Principal component analysis. Springer, Heidelberg
18. Kamvar S, Haveliwala T, Manning C, Golub G (2003) Exploiting the block structure of the web for computing pagerank. Stanford University Technical Report
19. Karypis G, Kumar V (1999) Parallel multilevel k-way partitioning for irregular graphs. *SIAM Rev* **41**(2), 278–300
20. Liben-Nowell D, Kleinberg J (2003) The link prediction problem for social networks. In: Proc. CIKM
21. Lu W, Janssen JCM, Milios EE, Japkowicz N, Zhang Y (2007) Node similarity in the citation graph. *J Knowledge Informat Syst* **11**(1), 105–129
22. Ng A, Jordan M, Weiss Y (2001) On spectral clustering: Analysis and an algorithm. In: NIPS, pp 849–856
23. Page L, Brin S, Motwani R, Winograd T (1998) The PageRank citation ranking: Bringing order to the web. Technical Report, Stanford Digital Library Technologies Project. Paper SIDL-WP-1999-0120 (version of 11/11/1999)
24. Palopoli L, Rosaci D, Terracina G, Ursino D (2005) A graph-based approach for extracting terminological properties from information sources with heterogeneous formats. *J Knowledge Informat Syst* **8**(4), 462–497
25. Pan J-Y, Yang H-J, Faloutsos C, Duygulu P (2004) Automatic multimedia cross-modal correlation discovery. In: KDD, pp 653–658
26. Piegorsch W, Casella GE (1990) Inverting a sum of matrices. *SIAM Rev* **32**:470
27. Rasmussen CE, Williams C (2006) Gaussian processes for machine learning. MIT Press
28. Sun J, Qu H, Chakrabarti D, Faloutsos C (2005) Neighborhood formation and anomaly detection in bipartite graphs. In: ICDM, pp 418–425
29. Tong H, Faloutsos C (2006) Center-piece subgraphs: Problem definition and fast solutions. In: KDD
30. Zhou D, Bousquet O, Lal TN, Weston J, Scholkopf B (2003) Learning with local and global consistency. In: NIPS
31. Zhu X, Ghahramani Z, Lafferty JD (2003) Semi-supervised learning using gaussian field and harmonic functions. In: ICML, pp 912–919

## Authors Biography



**Hanghang Tong** is a Ph.D. student at School of Computer Science, Carnegie Mellon University. He has received “best research paper” from ICDM 2006. He received a M.S. degree and a B.S. degree from Tsinghua University, P.R. China. His research interest includes data mining for multimedia and graphs.



**Christos Faloutsos** is a Professor at Carnegie Mellon University. He has received the Presidential Young Investigator Award by the National Science Foundation (1989), the Research Contributions Award in ICDM 2006, ten “best paper” awards, and several teaching awards. He has served as a member of the executive committee of SIG-KDD; he has published over 160 refereed articles, 11 book chapters and one monograph. He holds five patents and he has given over 20 tutorials and 10 invited distinguished lectures. His research interests include data mining for streams and graphs, fractals, database performance, and indexing for multimedia and bio-informatics data.



**Jia-Yu Pan** received his Ph.D. degree from Carnegie Mellon University in 2006. He has received three best paper awards from the conferences ICDM 2006, ICDM 2005, and PAKDD 2004. He is now at Google Inc., Pittsburgh, USA. He received a M.S. degree from National Taiwan University and a B.S. degree from National Chiao Tung University, Taiwan. His research interests include data mining for multimedia and graphs, clustering, and anomaly detection.